



Islamic Azad University



Noise Equivalent Power Optimization of Graphene-Superconductor Optical Sensors in the Current Bias Mode

Ali Moftakharzadeh^{*1}, Behnaz Afkhami Aghda², Mehdi Hosseini³

¹ Department of Electrical Engineering, Yazd University, Yazd, Iran, Postal Code 89195-741.

² Pishgaman Asr Ertebatat Company, Yazd, Iran.

³ Department of physics, Shiraz University of Technology, Shiraz, Iran, Postal Code 313-71555.

(Received 21 Jun. 2018; Revised 19 Jul. 2018; Accepted 25 Aug. 2018; Published 15 Sep. 2018)

Abstract: In this paper, the noise equivalent power (NEP) of an optical sensor based on graphene-superconductor junctions in the constant current mode of operation has been calculated. Furthermore, the necessary investigations to optimize the device noise with respect to various parameters such as the operating temperature, magnetic field, device resistance, voltage and current bias have been presented. By simultaneously solving the free energy and charge carrier density equations of graphene at low temperature, the specific heat, thermal interaction of electron-phonon and current responsivity of the sensor have been calculated. Using these parameters, the noise equivalent power of the device has been obtained. The results show that the behavior of device NEP by increasing the magnetic field at a constant temperature is at first ascending and then descending. The NEP value for different temperatures, up to $T=80\text{K}$, has an increasing behavior and then by further increasing the temperature, the NEP will show decreasing behavior which is also dependent on the value of the magnetic field. The NEP value is directly related to the device voltage and current values, therefore by increasing the voltage and current, the NEP will increase. Our investigations show that at the constant current bias mode of operation, the final device NEP is independent of the device resistance.

Keywords: Graphene, Noise Equivalent Power (NEP), Optical Sensors, Superconductor.

1. INTRODUCTION

Recently, fabrication of a single layer two-dimensional carbon atoms with honeycomb lattice which is called graphene has introduced a new structure with unique properties. Graphene was experimentally fabricated by Novoselov group

* Corresponding author. Email: moftakharzadeh@yazd.ac.ir

in 2004 [1-3].

Graphene has a quasi-metal band structure with a zero energy band gap and a linear dispersion relation at low temperatures which leads to a completely different behavior compared to semiconductors and conductors. In fact, electrons in graphene behave like two-dimensional Dirac fermions with zero mass [4-6]. Some quantum transport phenomena like integer quantum Hall effect [2, 3, 7], Conductance quantization [8] and Sub-Poissonian shot noise [9] have been studied in graphene and unusual characteristics result from quasi-relativistic dynamics have been observed. The effects of a strong electrical field [10], Klein tunneling [11] and induced superconductivity in graphene have also attracted many interests. Induction of the superconductivity in graphene is possible through the proximity effect by placing a superconductor electrode on graphene [12-14]. On the other hand, optical detectors have an important role in sensitive technologies [15-17]. Optical detectors are mostly fabricated using semiconductor materials in the visible wavelengths. On the other hand, superconductor material and graphene beside quantum wells are suitable candidates to fabricate high responsivity detectors in the far-infrared and terahertz wavelengths [18-23].

Graphene also has very interesting optical properties such as a constant optical conductance in the infrared range, a controllable optical absorption using the gate, an adjustable gap, etc. These properties made graphene a suitable material for designing infrared detectors and lasers [24, 25].

In recent years, the properties of graphene in proximity to semiconductors, superconductors and ferromagnetic materials have attracted a lot of interests [12-14, 26]. For the first time, Beenakker has studied conductance of a normal-superconductor junction based on graphene and has reported the specular Andreev reflection in graphene [12].

In this paper, an optical sensor base on a superconductor-graphene junction has been investigated and the noise parameters of this detector have been studied. The optical response of the sensor at a constant bias current has been investigated by calculation of thermodynamic and magnetic parameters of graphene at low temperatures. Then the noise equivalent power (NEP) of the device is calculated, and the effect of different parameters on the NEP has been investigated.

2. THEORETICAL DETAILS

The system consisting of a superconductor-graphene junction has been depicted in Fig. 1. The noise equivalent power of this system can be obtained using (1) [27].

$$NEP_{total}^2 = \frac{\langle \delta V_{\omega}^2 \rangle_{amp}}{S_V^2(0, I)} + 10k_B \Sigma \nu (T_e^6 + T_{ph}^6) + NEP_{NIS}^2 \quad (1)$$

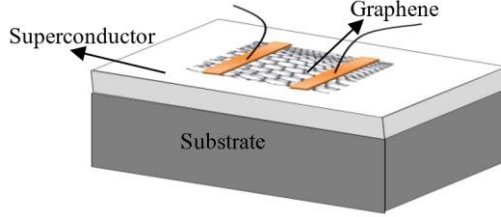


Fig. 1. Structure of the graphene-superconductor optical sensor.

According to (1), the NEP is the sum of three components in which $\langle \delta V_{\omega}^2 \rangle_{amp}$ is the voltage sensitivity of the SQUID amplifier, and NEP_{NIS} is the noise of the superconductor-insulator-normal junction and is calculated using (2) [27]:

$$NEP_{NIS}^2 = \langle \delta P_{\omega}^2 \rangle - 2 \frac{\langle \delta P_{\omega} \delta I_{\omega} \rangle}{\frac{\partial I}{\partial V} S_V(0, I)} + \frac{\langle \delta I_{\omega}^2 \rangle}{\left(\frac{\partial I}{\partial V} S_V(0, I) \right)^2} \quad (2)$$

The second term of (1) is the noise related to the electron-phonon flux current. Under equilibrium condition ($T_e = T_{ph} = T$), this term can be simplified as:

$$T_e = T_{ph} \Rightarrow 10k_B \Sigma \nu (T_e^6 + T_{ph}^6) \approx 4k_B G_{e-ph} T^2 \quad (3)$$

By using the detailed calculation of graphene thermodynamic properties from [28] and [29], the thermal conductance of the electron-phonon interaction is calculated as follows:

$$G_{e-ph} \approx \left(\left[\frac{1.373B^2}{n_0 \phi_0^2} + \frac{0.343B}{\phi_0} \right] \mu - 0.414n_0 \right) \frac{\nu l}{3} \frac{k_B \mu}{V_m} e^{-0.41\mu}. \quad (4)$$

In which $\mu = \frac{\gamma_1}{k_B T} \alpha \sqrt{B}$.

As it is obvious from (1), the total NEP is also dependent on the device responsivity. So by considering the constant bias current mode of operation, the voltage response of the detector can be calculated using (5) [26]:

$$S_V(\omega, I) = \frac{\delta V_{\omega}}{\delta P_{\omega}} = \frac{-(\partial I / \partial T) / (\partial I / \partial V)}{-i \alpha c_{\nu} \nu + 5 \Sigma \nu T_e^4 + \frac{\partial P}{\partial T} - \frac{(\partial I / \partial T)}{(\partial I / \partial V)} \frac{\partial P}{\partial V}} \quad (5)$$

In which:

$$-\frac{(\partial I/\partial T)}{(\partial I/\partial V)} = -\frac{k_B}{e} \left(\ln \frac{\sqrt{2\pi\Delta k_B T_e} + 1}{2eIR} \right), \quad (6)$$

$$\frac{\partial P}{\partial T} - \frac{(\partial I/\partial T)}{(\partial I/\partial V)} \frac{\partial P}{\partial T} = I \frac{k_B}{e} \left(\ln \frac{\sqrt{2\pi\Delta k_B T_e} + 1}{2eIR} + \frac{1}{2} \right).$$

and $5\Sigma\nu T_e^4$ is the thermal conductance of the electron-phonon interaction (G_{e-ph}) in graphene.

Assuming low chopping frequency and free-standing approximation ($G_{NIS} \gg G_{e-ph}$) and using (4), (5), and (6), the voltage response of the detector is calculated as:

$$S_V(\omega, I) = \frac{-\frac{k_B}{e} \left(\ln \frac{\sqrt{2\pi\Delta k_B T_e} + 1}{2eIR} \right)}{\frac{1}{3}vl \left(\left[1.373 \frac{B^2}{n_0\phi_0^2} + 0.343 \frac{B}{\phi_0} \right] \mu - 0.414n_0 \right) k_B \mu e^{-(\sqrt{2}-1)\mu} + I \frac{k_B}{e} \left(\ln \frac{\sqrt{2\pi\Delta k_B T_e} + 1}{2eIR} + \frac{1}{2} \right)} \quad (7)$$

It should be noted that in the bias current mode of operation, by biasing the device using a constant current, the change in the voltage of the device is measured as the device response. In this mode if the voltage changes are in the range of $k_B T_e < eV < \Delta - k_B T$ (in which $\Delta = 174\mu\text{eV}$), then the device current and voltage are related by (8).

$$I = \sqrt{\pi\Delta k_B T} / \left(\sqrt{2eR} \right) e^{\frac{\Delta - eV}{k_B T}} \Rightarrow eV = \Delta + k_B T \ln \left(\sqrt{2eRI} / \sqrt{\pi\Delta k_B T} \right) \quad (8)$$

After calculation of the voltage response as a function of the bias current, the NEP of the device can be obtained. Using (4), the resulting NEP from the electron-phonon interaction is calculated in (9). (This parameter has been normalized with respect to the molar volume.)

$$NEP_{e-ph}^2 = \frac{4}{3}vl \left(\left[1.373 \frac{B^2}{n_0\phi_0^2} + 0.343 \frac{B}{\phi_0} \right] \mu - 0.414n_0 \right) \times k_B^2 T^2 \mu e^{-(\sqrt{2}-1)\mu}. \quad (9)$$

The noise related to the NIS junction has been calculated using (2) and aforementioned approximations which is presented in (10) [26].

$$\langle \delta P_\omega^2 \rangle \approx \left(A^2 + \frac{1}{2} \right) (k_B T_e)^2 I / e \quad (10)$$

$$\langle \delta P_\omega \delta I_\omega \rangle \approx 2eP \approx 2k_B T_e I \left(A - \frac{1}{2} \right), \quad \langle \delta I_\omega^2 \rangle = 2eI,$$

in which:

$$A = \ln \frac{\sqrt{2\pi\Delta k_B T_e}}{2eIR} + \frac{1}{2}. \quad (11)$$

And the derivative of the current with respect to the voltage can be calculated using (8).

$$NEP_{NIS}^2 = \left[\left(\ln \frac{\sqrt{2\pi\Delta k_B T_e}}{2eIR} + \frac{1}{2} \right)^2 + \frac{1}{2} \right] \frac{(k_B T_e)^2 I}{e} - \frac{4k_B T_e I \left[\left(\ln \frac{\sqrt{2\pi\Delta k_B T_e}}{2eIR} + \frac{1}{2} \right) - \frac{1}{2} \right]}{\left(\frac{\sqrt{\pi\Delta k_B T_e}}{\sqrt{2eR}} \frac{e}{k_B T_e} e^{-\frac{\Delta-eV}{k_B T_e}} \right) \times S} + \frac{2eI}{\left[\left(\frac{\sqrt{\pi\Delta k_B T_e}}{\sqrt{2eR}} \frac{e}{k_B T_e} e^{-\frac{\Delta-eV}{k_B T_e}} \right) \times S \right]^2} \quad (12)$$

Finally, considering (1) and by using (7), (9), and (12) the total NEP of the device is obtained.

3. RESULTS AND DISCUSSIONS

At first, effects of the magnetic field and the operating temperature of the device on the total NEP have been investigated. Only the trend of the effect of these parameters is investigated, therefore all plots have been normalized.

The normalized device NEP versus the magnetic field and the operating temperature has been plotted in Fig. 2. As it is shown in Fig. 2(a), the device NEP versus magnetic field has a maximum point which is not a suitable operation point for these types of detectors and should be avoided. At low temperatures, the speed of reaching the maximum point is higher and so the maximum point is at lower values of the magnetic field. At low temperatures, the device NEP will decline rapidly after reaching its maximum value. The slope of reduction of NEP is smaller at higher temperatures. So that at $T=80K$, the value of NEP is almost constant after reaching its maximum value.

The normalized NEP versus device temperature at different magnetic fields is presented in Fig. 2(b). As it is shown in this figure, the NEP value will start to increase after $T=10K$. Also, the NEP versus temperature has a higher incremental slope at low values of the magnetic field. It should be noted that the device NEP is almost independent of the magnetic field at high values of the operating temperature beyond $T=80K$. So, it can be deduced that at high values of device temperature the dominant part in device noise is the noise related to the electron-phonon interaction (The second part in (1)).

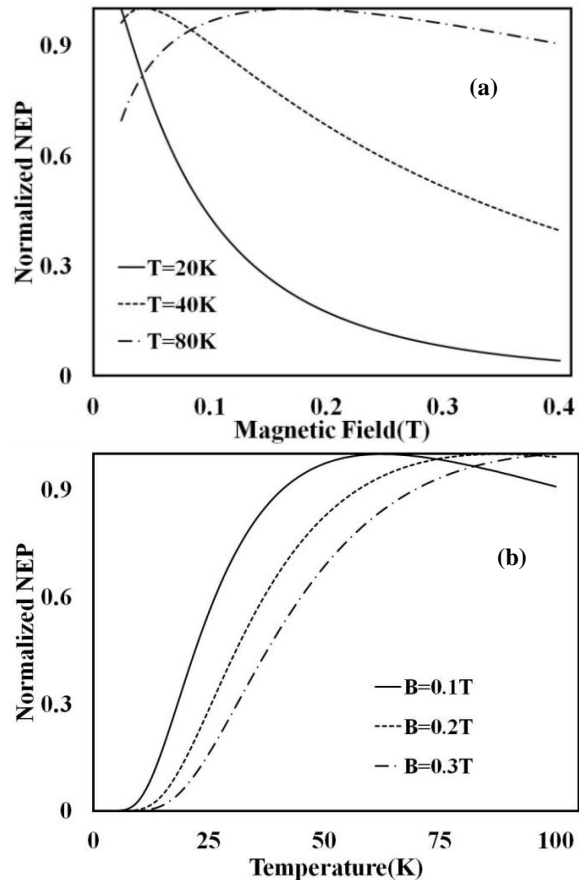


Fig. 2. (a) Normalized NEP versus magnetic field at different operating temperatures. (b) Normalized NEP versus temperature at different magnetic fields. The following values have been considered in plotting of this figure: device resistance = 1Ω , device voltage = $100\ \mu\text{V}$, $\langle \delta V_{\omega}^2 \rangle_{amp} = 3\text{nV} / \sqrt{\text{Hz}}$ and $G_{NIS} = 1.5 \times 10^{-13}$.

As it is previously mentioned, for calculation of the device NEP a specific operating voltage range has been considered. Fig. 3 has been plotted to further investigate the effect of the device voltage on the total device NEP.

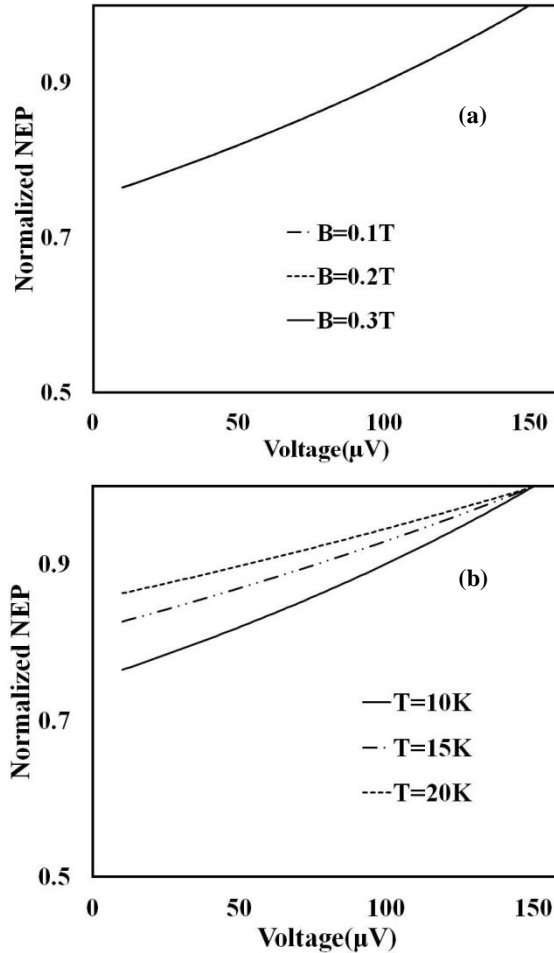


Fig. 3. (a) Normalized NEP versus voltage at different magnetic field and temperature of 10K. (b) Normalized NEP versus voltage at different temperatures and magnetic field of 0.3T. The device resistance is 1Ω.

In Fig. 3(a), the device NEP versus voltage at a specific temperature and a constant device resistance is shown using different values for the magnetic field. In general, increasing the device voltage will result in the enhancement of the device NEP. As it is obvious in this figure, the normalized device NEP is independent of the magnetic field. This is due to the fact that the voltage dependent terms in the NEP calculation are independent of the magnetic field, so the normalization will cancel out the effect of the magnetic field.

The NEP versus voltage at a predetermined magnetic field and a constant device resistance and for different values of operating temperature is drawn in

Fig. 3(b). Generally, this figure shows that the increment of the device voltage will result in the enhancement of device NEP, but the amount and style of this enhancement are dependent on the device temperature. The slope and the amount of this increment in the device NEP are higher at low temperatures. Also, by increasing the device temperature, the variation in the device NEP by changing the device voltage is smaller. Furthermore, it can be observed that at a constant voltage, the NEP has a direct relationship with the device temperature. So, increasing the device temperature will increase the device NEP.

Another important device parameter in the NEP calculation is the bias current which itself depends on the operation temperature. Fig. 4 reveals the NEP versus bias current for different values of magnetic field at the temperature of 10K. Due to the dependency of the bias current on the operating temperature, the behavior of NEP in Fig. 4 is similar to Fig. 2(b). At the very small amount of bias current the NEP is very small and by increasing the bias current the NEP will increase rapidly. As it is shown, at the bias current of 1.5mA, the value of NEP will start to reduce and by enhancing the magnetic field the slope of this reduction will decrease. So that at $B=0.3\text{T}$, the NEP will be almost constant for the bias current greater than 1.5mA. It is worth mentioning that at higher values of the magnetic field the starting enhancement point of the device NEP will shift toward higher values of the bias current. As it is obvious from Fig. 4, the practical value of the bias current should be smaller than 1.5mA due to high NEP values at higher bias currents.

The figures 2, 3 and 4 show that there is a point with special values of magnetic field, operating temperature and bias current in which the NEP is maximum and by going away from this point the NEP will decrease.

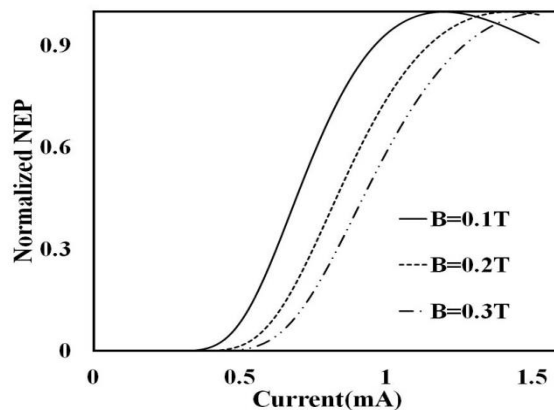


Fig. 4. Normalized NEP versus bias current at different magnetic fields. The device resistance is assumed to be 1Ω .

4. CONCLUSION

The results show that the device NEP versus magnetic field has a maximum point which should be avoided for the better performance of the detector. It is also shown that by increasing the device temperature the value of NEP will increase and the style of this increment is dependent on different values of the magnetic field.

Our investigation on the effect of device voltage on the NEP shows that enhancement of the device voltage will increase the total NEP in general, but the amount of this enhancement is dependent on the device temperature and the magnetic field. At small values of temperature, enhancement of the device NEP is faster with a larger incremental slope.

The device NEP has a direct relationship with the bias current. The device NEP is higher for higher values of the bias current, so by choosing smaller values of the bias current the NEP of the device can be reduced.

REFERENCES

- [1] K. S. Novoselov, A. K. Geim, S. V. Morozov, D. Jiang, Y. Zhang, S. V. Dubonos, I. V. Grigorieva, and A. A. Firsov. *Electric field effect in atomically thin carbon films*. Science. [Online]. 306(5696) (2004, Oct.) 666-669.
Available: <http://science.sciencemag.org/content/306/5696/666>
- [2] K. S. Novoselov, A. K. Geim, S. V. Morozov, D. Jiang, M. I. Katsnelson, I. V. Grigorieva, S. V. Dubonos, and A. A. Firsov. *Two-dimensional gas of massless Dirac fermions in graphene*. Nature. [Online]. 438 (2005, Nov.) 197-200.
Available: <https://www.nature.com/articles/nature04233>
- [3] Y. Zhang, Y. W. Tan, H. L. Stormer, and P. Kim. *Experimental observation of the quantum Hall Effect and Berry's phase in graphene*. Nature. [Online]. 438 (2005, Nov.) 201-204. Available: <https://www.nature.com/articles/nature04235>
- [4] P. R. Wallace. *The band theory of graphite*. Phys. Rev. 71(9) (1947, May.) 622-634.
- [5] J. C. Slonczewski, and P. R. Weiss. *Band structure of graphite*. Phys. Rev. 109(2) (1958, Jan.) 272-279.
- [6] G. W. Semenoff. *Condensed-matter simulation of a three-dimensional anomaly*. Phys. Rev. Lett. [Online]. 53(26) (1984, Dec.) 2449-2452.
Available: <https://journals.aps.org/prl/abstract/10.1103/PhysRevLett.53.2449>
- [7] V. P. Gusynin, and S. G. Sharapov. *Unconventional integer quantum Hall effect in graphene*. Phys. Rev. Lett. [Online]. 95(14) (2005, Sep.) 146801.
Available: <https://journals.aps.org/prl/abstract/10.1103/PhysRevLett.95.146801>
- [8] N. M. R. Peres, A. H. Castro Neto, and F. Guinea. *Conductance quantization in mesoscopic graphene*. Phys. Rev. B. [Online]. 73(19) (2006, May.) 195411.
Available: <https://journals.aps.org/prb/abstract/10.1103/PhysRevB.73.195411>

- [9] J. Tworzydło, B. Trauzettel, M. Titov, A. Rycerz, and C. W. Beenakker. *Sub-Poissonian shot noise in graphene*. Phys. Rev. Lett. [Online]. 96(24) (2006, Jun.) 246802.
Available: <https://journals.aps.org/prl/abstract/10.1103/PhysRevLett.96.246802>
- [10] Y. Zhang, J. P. Small, M. E. Amori, and P. Kim. *Electric field modulation of galvanomagnetic properties of mesoscopic graphite*. Phys. Rev. Lett. [Online]. 94(17) (2005, May.) 176803.
Available: <https://journals.aps.org/prl/abstract/10.1103/PhysRevLett.94.176803>
- [11] M. I. Katsnelson, K. S. Novoselov, and A. K. Geim. *Chiral tunneling and the Klein paradox in graphene*. Nature physics. [Online]. 2(9) (2006, Aug.) 620-625.
Available: <https://www.nature.com/articles/nphys384>
- [12] C. W. J. Beenaker. *Specular Andreev Reflection in Graphene*. Phys. Rev. Lett. [Online]. 97 (2006, Aug.) 067007.
Available: <https://journals.aps.org/prl/abstract/10.1103/PhysRevLett.97.067007>
- [13] A. F. Volkov, P. H. C. Magnée, B. J. Van Wees, and T. M. Klapwijk. *Proximity and Josephson effects in superconductor-two-dimensional electron gas planar junctions*. Physica C: Superconductivity. [Online]. 242(3) (1995, Feb.) 261-266.
Available: <https://www.sciencedirect.com/science/article/abs/pii/0921453494024294>
- [14] M. Titov, and C. W. Beenakker. *Josephson effect in ballistic graphene*. Phys. Rev. B. [Online]. 74(4) (2006, Jul.) 041401.
Available: <https://journals.aps.org/prb/abstract/10.1103/PhysRevB.74.041401>
- [15] P. W. Barone, S. Baik, D. A. Heller, and M. S. Strano. *Near-infrared optical sensors based on single-walled carbon nanotubes*. Nature Materials. [Online]. 4 (2005, Dec.) 86-92. Available: <https://www.nature.com/articles/nmat1276>
- [16] J. Lou, Y. Wang, and L. Tong. *Microfiber optical sensors: A review*. Sensors. [Online]. 14(4) (2014, Mar.) 5823-5844.
Available: <https://www.ncbi.nlm.nih.gov/pmc/articles/PMC4029688/>
- [17] A., Dinoi, A. Donato, F. Belosi, M. Conte, and D. Contini. "Comparison of atmospheric particle concentration measurements using different optical detectors: Potentiality and limits for air quality applications." Measurement 106 (2017): 274-282.
- [18] R. J. Keyes. *Optical and infrared detector*. 2nd ed. Springer Science & Business Media (2013), 101-147.
- [19] F. Alves, D. Grbovic, and G. Karunasiri, February. *MEMS THz sensors using metasurface structures*. "In Terahertz, RF, Millimeter, and Submillimeter-Wave Technology and Applications XI." International Society for Optics and Photonics. 10531 (2018) 1053111.
Available: <http://iopscience.iop.org/article/10.1088/0953-2048/9/10/001>

- [20] Z. Chen, G., Hefferman, and T. Wei,. “A low bandwidth DFB laser-based interrogator for terahertz-range fiber Bragg grating sensors.” *IEEE Photonics Technology Letters*, (2017), 29(4), pp.365-368.
- [21] M. Hosseini, A. Moftakharzadeh, A. Kokabi, M. A. Vesaghi, H. Kinder, and M. Fardmanesh. *Characterization of a transition-edge bolometer made of YBCO thin films prepared by nonfluorine metal–organic deposition*. *IEEE Trans. on Appl. Supercond.* [Online]. 21(6) (2011, Dec.) 3587-3591.
Available: <https://ieeexplore.ieee.org/document/6029287/>
- [22] M. Hosseini, A. Kokabi, A. Moftakharzadeh, M. A. Vesaghi, and M. Fardmanesh. *Effect of substrate thickness on responsivity of free-membrane bolometric detectors*. *IEEE Sensors Journal*. [Online]. 11(12) (2011, May.) 3283-3287.
Available: <https://ieeexplore.ieee.org/abstract/document/5772900/>
- [23] M. Hosseini. *Tailoring the terahertz absorption in the quantum wells*. *Optik-International Journal for Light and Electron Optics*. [Online]. 127(10) (2016, May.) 4554-4558.
Available: <https://www.sciencedirect.com/science/article/pii/S0030402616002072>
- [24] J. Fernández-Rossier, J. J. Palacios, and L. Brey. *Electronic structure of gated graphene and graphene ribbons*. *Phys. Rev. B*. [Online]. 75 (2007, May.) 205441.
Available: <https://journals.aps.org/prb/abstract/10.1103/PhysRevB.75.205441>
- [25] M. S. Azadeh, A. Kokabi, M. Hosseini, and M. Fardmanesh. *Tunable bandgap opening in the proposed structure of silicon-doped graphene*. *Micro & Nano Lett.* [Online]. 6(8) (2011, Aug.) 582-585.
Available: <https://ieeexplore.ieee.org/document/6012991/>
- [26] M. B. Shalom, M. J. Zhu, V. I. Fal’ko, A. Mishchenko, A. V. Kretinin, K. S. Novoselov, C. R. Woods K. Watanabe, T. Taniguchi, A. K. Geim, and J. R. Prance. *Quantum oscillations of the critical current and high-field superconducting proximity in ballistic graphene*. *Nature Physics*. [Online]. 12(4) (2016, Dec.) 318-322. Available: <https://www.nature.com/articles/nphys3592>
- [27] D. Golubev and L. Kuzmin. *Nonequilibrium theory of a hot-electron bolometer with normal metal-insulatorsuperconductor tunnel junction*. *Journal of Applied Physics*. [Online]. 89(11) (2001, Jun.) 6464-6472.
Available: <https://aip.scitation.org/doi/abs/10.1063/1.1351002>
- [28] B. A. Aghda, A. Moftakharzadeh, and M. Hosseini. *Noise Equivalent Power of Graphene–Superconductor-Based Optical Sensor*. *Fluctuation and Noise Letters*. [Online]. 16(01) (2017, Mar.) 1750006.
Available: <https://www.worldscientific.com/doi/abs/10.1142/S0219477517500067>
- [29] B. V. Duppen and F. M. Peeters. *Thermodynamic properties of the electron gas in multilayer graphene in the presence of a perpendicular magnetic field*. *Phys. Rev. B*. [Online]. 88(24) (2013, Dec.) 245429.
Available: <https://journals.aps.org/prb/abstract/10.1103/PhysRevB.88.245429>

